HHS Public Access
Author manuscript
Signal Processing. Author manuscript; available in PMC 2019 July 09.

Published in final edited form as:
Signal Processing. 2018 August ; 149: 27–35. doi:10.1016/j.sigpro.2018.02.025.

Active contours driven by edge entropy fitting energy for image segmentation

Lei Wang[a,b], **Guangqiang Chen**[c], **Dai Shi**[c], **Yan Chang**[a], **Sixian Chan**[d], **Jiantao Pu**[b,*], and **Xiaodong Yang**[a,*]

[a]Medical Imaging Department, Suzhou Institute of Biomedical Engineering and Technology, Chinese Academy of Sciences, Suzhou, China

[b]Departments of Radiology and Bioengineering, University of Pittsburgh, Pittsburgh, USA

[c]Department of Radiology, The Second Affiliated Hospital of Soochow University, Suzhou, China

[d]College of Computer Science and Technology, Zhejiang University of Technology, Hangzhou, China

Abstract

Active contour models have been widely used for image segmentation purposes. However, they may fail to delineate objects of interest depicted on images with intensity inhomogeneity. To resolve this issue, a novel image feature, termed as local edge entropy, is proposed in this study to reduce the negative impact of inhomogeneity on image segmentation. An active contour model is developed on the basis of this feature, where an edge entropy fitting (EEF) energy is defined with the combination of a redesigned regularization term. Minimizing the energy in a variational level set formulation can successfully drive the motion of an initial contour curve towards optimal object boundaries. Experiments on a number of test images demonstrate that the proposed model has the capability of handling intensity inhomogeneity with reasonable segmentation accuracy.

Keywords

Image segmentation; Active contour models; Intensity inhomogeneity; Local edge entropy

1. Introduction

Image segmentation [1] aims to partition an image into meaningful subregions. There have been numerous approaches developed for this purpose [2–4]. Among the available schemes, active contour models [5–7] attract considerable attention and are able to segment target regions with reasonable accuracy. The underlying idea of the active contour models is initializing a contour as the zero level set [8] of a higher dimensional function and then driving the contour towards object boundaries by minimizing a predefined energy functional. To minimize the energy, a variational level set formulation is widely used to deal with

*Corresponding authors. jip13@pitt.edu (J. Pu), xiaodong.yang@sibet.ac.cn (X. Yang).

topological changes of contour curves. The available active contour models can be primarily categorized into edge based models [9,10] and region based models [11–13].

Edge based models generally segment images by introducing image gradients as an edge stopping function (ESF) [6] into a predefined energy functional. Their advantages are the low computational cost and reliable segmentation performance for objects with high contrast; however, they are sensitive to the presence of noise and intensity inhomogeneity. Consequently, this type of models cannot work well for images with obvious noisy and inhomogeneous intensity, tends to get stuck in local minima and may suffer from leakage problems in weak boundary regions. To overcome these disadvantages, region based models have been developed to statistically model desirable object regions. Although they are relatively robust against image noise and initial contour placements, they may fail to segment images with intensity inhomogeneity because they are theoretically based on a homogeneous assumption that different objects have different intensities.

To enable a reliable segmentation for images with inhomogeneous intensity, a number of feature information has been utilized to guide the optimal evolution of contour curves [14]. He et al. [15] improved the region-scalable fitting (RSF) energy [16] by assigning each pixel with a homogeneous weight derived from local grey level distribution entropy and replacing Gaussian kernel with a mollifying kernel, termed as the WRSF model. Dai et al. [17] developed an inhomogeneity-embedded (InH) active contour model by introducing a pixel inhomogeneity factor into the model originally proposed by Chan and Vese (CV) [6] for natural image segmentation. Unlike the InH model, Niu et al. [18] extended the CV model (ECV) by characterizing local image differences between pixel coordinates and intensities. These models demonstrated a reasonable performance in handling intensity inhomogeneity, but the utilized feature information may be insufficient to alleviate the influence of intensity inhomogeneity for certain images and ultimately fail to differentiate the foreground and background as illustrated by the example in Fig. 1. Hence, it is desirable to develop novel image segmentation schemes that can significantly alleviate the influence of intensity inhomogeneity and thus enable a reliable and accurate delineation of the boundaries of objects depicted on images.

In this study, a novel region based model is proposed to effectively detect object boundaries in inhomogeneous regions and exclude irrelevant image background. Specifically, a new image feature, termed as local edge entropy, is introduced to suppress intensity inhomogeneity and highlight object edges in fuzzy regions. This entropy is large in regions containing edge information, and can assist in differentiating the foreground from the background in segmentation. Based on the proposed edge entropy, a region based model is developed by extending the RSF energy function. The model aims to drive the evolution of the initial contours towards object boundaries with a high accuracy as compared to available models with only intensity information. In particular, a length regularization term of the level set function [6] is redefined based on the edge entropy to keep contour curves smooth and close to object boundaries. The regularization term aims to reduce unnecessary contour evolution and improve segmentation accuracy.

The remainder of this paper is organized as follows. Section 2 briefly presents an overview of two typical region based models and explains their advantages and weaknesses. Section 3 introduces the developed edge entropy and energy functional, along with the redesigned regularization term of the level set function. In Section 4, we describe the performance metrics and experimental results. Finally, we discussed the developed model and conclude this study respectively in Sections 5 and 6.

2. Related work

2.1. The CV model

The CV model [6] was originally proposed to mitigate the Mumfor-Shah problem [19] by assuming that the image to be processed was a piecewise constant function. Let $\Omega \subset \mathfrak{R}^2$ be a two-dimensional (2D) image domain, I: $\Omega \subset \mathfrak{R}$ be a gray image. For each pixel x in the image, the CV model can use constants c_1 and c_2 to globally characterize the intensity differences between the foreground and background based on the following fitting energy:

$$E^{CV} = \lambda_1 \int_{\Omega_1} \left|I(x) - c_1\right|^2 H_1(\phi)dx + \lambda_2 \int_{\Omega_2} \left|I(x) - c_2\right|^2 H_2(\phi)dx \quad (1)$$

where Ω_1 and Ω_2 denote the internal and external regions of a given initial contour C: $\Omega \subset \mathfrak{R}$. These two regions are specified by functions $H_1(\phi) = H(\phi)$ and $H_2(\phi) = 1 - H(\phi)$. respectively, where $H(\phi) = 0.5 + \arctan(\phi/\varepsilon)/\pi$ is the smoothed Heaviside function with a small positive constant ε. ϕ: $\Omega \subset \mathfrak{R}$ is the level set function to represent the initial contour C. Constants c_1 and c_2 are used to approximate pixel intensities in regions Ω_1 and Ω_2. λ_1 and λ_2 are nonnegative constants to balance two image fitting terms in the energy functional.

The CV model is relatively insensitive to image noise and the initial contour placements due to the presence of global intensities. However, it relies on the piecewise constant assumption and ignores other image information (*e.g.*, intensity means and variances) in local or global regions, and thus may lead to limited segmentation accuracy especially for images with inhomogeneous intensity. In addition, representing the image differences between the foreground and background by merely using constants c_1 and c_2 is not sufficient for accurate segmentation.

2.2. The RSF model

To lower the influence of inhomogeneity, the RSF model [16] was developed to extend the CV model by utilizing the local image information specified by a Gaussian window. The fitting energy of the model can be represented as:

$$\begin{aligned} E^{RSF} = \lambda_1 \iint K_\sigma(x, y)\left|I(y) - f_1(x)\right|^2 H_1(\phi)dydx \\ + \lambda_2 \iint K_\sigma(x, y)\left|I(y) - f_2(x)\right|^2 H_2(\phi)dydx \end{aligned} \quad (2)$$

where $K_\sigma(x, y) = \exp(-(x-y)^2/2\sigma^2)/\sqrt{2\pi}\sigma$ is the Gaussian window function with standard deviation σ. This function defines a local neighborhood centered at x and specifies a weight for each pixel y based on the distance between y and x; functions $f_1(x)$ and $f_2(x)$ approximately represent local pixel intensities inside and outside the contour curves, respectively. λ_1 and λ_2 are weighting parameters for two local image fitting terms.

Based on the RSF fitting energy and two level set regularization terms [16], this model is capable of correctly evolving the initial contour towards target boundaries, despite the presence of intensity inhomogeneity. It can also identify effectively small intensity differences in inhomogeneous regions and suppress irrelevant image background in segmentation. However, this model tends to fall into the local minima when the initial contour is far away from object boundaries. In addition, it ignores other useful image information in local or global regions, and thus leads to incomplete or even incorrect segmentation in noisy and inhomogeneous regions.

2.3. Summary

As demonstrated by the CV and RSF models, the region based models characterize the image differences inside and outside contour curves by merely utilizing pixel intensities in local or global regions. These intensities are simplified by different approximation functions *(e.g.,* c_i and $f_i(x)$), giving rise to the loss of valuable image information. This makes these models incompetent to suppress intensity inhomogeneity, and prone to improperly segment target objects depicted on inhomogeneous images. Hence, it may be prudent to utilize more image information to mitigate the adverse influence of inhomogeneity.

3. The proposed model based on edge entropy fitting energy

A novel region based model is proposed to segment images with intensity inhomogeneity. The model consists of three components: local edge entropy, edge entropy fitting energy functional, and redefined regularization term of the level set function. The local entropy is used to reduce the influence of inhomogeneity, while the functional and regularization term are used to differentiate the image differences between the foreground and the background of an object, and iteratively evolve the initial contours.

3.1. Local edge entropy

Image entropy has been widely used as an important feature in various image processing tasks, and can be expressed, based on the Shannon's definition [20], as follows:

$$L_r(x) = -\sum_{y \in \Pi_x} p(y)\log p(y) \qquad (3)$$

where Π_x is a local region centered at position x, with a diameter of r. $p(y)$ is a certain probability distribution of pixel y in the local region. The definition of $p(y)$ typically depends on the processing schemes for different tasks. In image segmentation, Shiozaki's definition [21,22] of $p(y) = I(y)/\sum_{j \in \Pi_x} I(j)$ is often used to stress intensity differences, and termed as local grey level distribution.

Image entropy based on local grey level distribution is related to intensity variation and has a large value for homogeneous regions and a small value for inhomogeneous regions [15]. This property can be used to reduce the influence of inhomogeneity. However, the range of this entropy is relatively small, leading to limited capability of identifying image differences in inhomogeneous regions, as shown in Fig. 2. To overcome the disadvantage, a novel probability distribution is proposed and defined as:

$$p(y) = \frac{\mathrm{mod}(I(y), m)}{m} \quad (4)$$

where m denotes the intensity mean in local region of Π_x; $mod(\cdot)$ is the modulus operator. With the proposed probability distribution, image entropy is large for edge regions and vice versa, and referred to as local edge entropy in this study. The unique property of edge entropy can be attributed to the use of local intensity mean. The statistical measure *(i.e., m)* makes the edge entropy relatively insensitive to the presence of image noise, and able to take values in a reasonable range. In addition, the statistical characteristic allows edge entropy to have a better capability of identifying intensity differences than the grey level distribution entropy and image gradient, in the presence of inhomogeneity.

3.2. Edge entropy fitting energy

According to the above analysis, the feature map of edge entropy can be regarded as a new image and incorporated into the RSF energy functional to assist in image segmentation. Thus, the edge entropy fitting (EEF) energy is constructed under the framework of the RSF model by simultaneously employing pixel intensity $I(x)$ and local edge entropy $L_r(x)$ to accurately segment objects of interest, and expressed as:

$$E^{EEF} = \sum_{i=1}^{2} \iint K_\sigma(x, y)\left[\left|I(y) - f_i(x)\right|^2 + \left|L_r(y) - m_i(x)\right|^2\right] \times H_i(\phi(y))dydx \quad (5)$$

where $L_r(y)$ denotes the edge entropy in the neighborhood of the position y with a diameter of r. r is set to 4 (pixels). $f_i(x)$ and $m_i(x)$ denote the intensity means for the images $I(x)$ and $L_r(x)$, respectively. These two images characterize objects of interest from different aspects and enable the EEF energy to differentiate the foreground and background.

To preserve the regularity of ϕ, two widely used regularization terms [13,18], namely $P(\phi)$ and $Q(\phi)$, are introduced into the developed energy to enable a stable and accurate evolution of the level set function:

$$P(\phi)=\frac{1}{2}\int(|\nabla\phi(x)-1|)^2dx \quad (6)$$

$$\mathrm{Q}(\phi)=\int\left|\nabla H(\phi(x))\right|dx \quad (7)$$

where $P(\phi)$ penalizes the deviation from a signed distance function, while $Q(\phi)$ enables the level set function to have an optimal length in contour evolution. ∇ is the gradient operator.

To keep the level set function close to object boundaries, the length regularization term $Q(\phi)$ is redefined as Q*(ϕ) to improve the computational efficiency and accuracy:

$$\mathrm{Q}*(\phi)=\int g(x)\left|\nabla H(\phi(x))\right|dx \quad (8)$$

where $g(x) = 1/(1 + L_r(x)^2)$ has a small value for edge regions and serves as an edge stopping function [23,24], which aims to reduce or stop the evolution of contour curves when they are close to object boundaries. By combining the two regularization terms and the EEF fitting energy, the final fitting energy functional is given by:

$$E(\phi)=E^{EEF}+\mu P(\phi)+\upsilon Q*(\phi) \quad (9)$$

where μ and υ are the weighting parameters for $P(\phi)$ and $Q*(\phi)$, respectively.

3.3. Energy functional minimization

To evolve the initial contours towards object boundaries, the proposed energy functional $E(\phi)$ needs to be minimized using the standard gradient descent method. For a fixed level set function φ, $E(\varphi)$ is minimized with respect to the functions $f_i(x)$ and $m_i(x)$, which satisfy the following equations separately:

$$\int K_\sigma(x,y)\big(I(y)-f_i(x)\big)H_i(\phi(y))dy=0 \quad (10)$$

$$\int K_\sigma(x,y)\big(L_r(y)-m_i(x)\big)H_i(\phi(y))dy=0 \quad (11)$$

Based on the above two equations, $f_i(x)$ and $m_i(x)$ are given by:

$$f_i(x) = \frac{\int K_\sigma(x,y) I(y) H_i(\phi(y)) dy}{\int K_\sigma(x,y) H_i(\phi(y)) dy} \quad (12)$$

$$m_i(x) = \frac{\int K_\sigma(x,y) L_r(y) H_i(\phi(y)) dy}{\int K_\sigma(x,y) H_i(\phi(y)) dy} \quad (13)$$

Keeping $f_i(x)$ and $m_i(x)$ fixed, $E(\phi)$ is minimized with respect to ϕ, resulting in the evolution formula of the level set function ϕ:

$$\begin{aligned}\frac{\partial \phi}{\partial t} = & -\delta(\phi)\left(e_1(x) - e_2(x)\right) + \mu\left(\nabla^2 \phi - div\left(\frac{\nabla \phi}{|\nabla \phi|}\right)\right) \\ & + \upsilon \delta(\phi) div\left(g(x) \frac{\nabla \phi}{|\nabla \phi|}\right)\end{aligned} \quad (14)$$

$$\begin{aligned} e_i(x) = & \int K_\sigma(x,y)\left(\left|I(y) - f_i(x)\right|^2 + \left|L_r(y) - m_i(x)\right|^2\right) dy, \\ & i = 1, 2 \end{aligned} \quad (15)$$

where $\delta(\varphi)$ is the derivative of the function $H(\varphi)$, $div(\cdot)$ denotes the divergence operator, and $e_i(x)$ simultaneously quantifies the image differences between the foreground and background for the original image and its edge entropy.

In contour evolution, the level set function φ was initially assigned to a positive constant 2 outside a region and −2 inside, and then updated iteratively by using the formulation of $\varphi^{n+1} = \varphi^n + \Delta t \cdot \Delta \varphi^n$ with iterative number n and the time step Δt. The convergence condition was $|\varphi^{n+1} - \varphi^n| \le \zeta$, where $\zeta = 0.1$ in this study [25]. σ was assigned to 3 to balance the convergence rate and computational efficiency. Gaussian window $K_\sigma(x, y)$ was simplified as a $(4\sigma + 1) \times (4\sigma + 1)$ mask as recommended in previous studies [11,26]. Δt and μ were related by $\Delta t \cdot \mu = 0.1$ to satisfy the Courant Friedrichs Lewy (CFL) condition for numerical stability [27] and they were set at $\Delta t = 0.1$ and $\mu = 1$, respectively. The parameter υ was set by default as $\upsilon = 0.001 \times 255 \times 255$.

4. Experiments

To demonstrate the performances of the proposed method, we performed segmentation experiments on a synthetic image dataset and a public Berkeley segmentation dataset 500 (BSDS500) [28]. The former, which can be accessed at http://www.engr.uconn.edu/~cmli/, was used widely in previous studies [16, 26], while the latter consists of a number of natural images and manual annotations. Experiment results are quantitatively estimated based on the Dice Similarity Coefficient (DSC) [29,30] that is defined as:

$$DSC(A,B) = \frac{2N(A \cap B)}{N(A) + N(B)} \quad (16)$$

where A denotes the results of a specific segmentation algorithm and B is the ground truth. ∩ is the intersection operator; $N(\cdot)$ indicates the number of pixels enclosed set. The DSC ranges from 0 to 1, and a higher DSC means a better segmentation performance.

4.1. Segmentation results

Figs. 3 and 4 showed the segmentation results when the proposed method was applied with different initial contour placements and image noise. It can be seen that the developed method successfully delineated the objects of interest, where the initial triangle, rectangle, pentagon and circle contours converged to the same results. As demonstrated by Fig. 4, the developed method can achieve consistent segmentation results for the images corrupted by additive Gaussian noise with the standard deviations of 5, 10, and 15, respectively, suggesting that the developed method was, to some extent, insensitive to initial contour placements and image noise.

Fig. 5 showed the segmentation results when the proposed method was applied to eight synthetic images with different intensity inhomogeneity and image noise. The developed method successfully identified the desirable objects with varying dimensions and shapes, and the average DSC was 0.935, suggesting a capability of dealing with intensity inhomogeneity with reasonable segmentation accuracy.

4.2. Performance comparison

We compared the performance of the proposed method with the CV, RSF, WRSF, InH and ECV methods using the above synthetic images (Figs. 5–7). It can be seen that the CV model had the smallest DSC values for the inhomogeneous images and failed to segment the objects of interest due to the mere use of global intensity information. The RSF model achieved a relatively good segmentation accuracy by using local intensities to identify image differences between the foreground and background, but it was not competent to locate target objects from inhomogeneity regions. Unlike the CV and RSF models, the other four methods took pixel intensities and feature information in local regions into account simultaneously to evolve the initial contours. Given their capability of dealing with intensity inhomogeneity, these four methods *(i.e.,* WRSF, InH, ECV and EEF) achieved high accuracy in terms of the average DSC *(i.e.,* 0.908, 0.923, 0.914 and 0.935) as compared to the CV and RSF methods *(i.e.,* 0.656 and 0.878).

The proposed method was further compared quantitatively with the RSF, WRSF, InH, and ECV methods using 35 randomly chosen natural images from the BSDS500 dataset. Experiment results of these methods were displayed in Fig. 8 where a box plot was used (25% for top limit and 75% for bottom, red line for the median value) based on the DSC metric. The DSC means of the RSF, WRSF, InH, ECV and our methods were 0.743, 0.781, 0.809, 0.776 and 0.812 with the standard deviations of 0.087, 0.073, 0.068, 0.077 and 0.066, respectively. The results demonstrated that the developed method had better segmentation performance in accuracy as compared with the other four methods (Fig. 9), and was capable of consistently delineating the objects of interest in the presence of inhomogeneous and complex background.

The computational cost of the above five methods was also assessed (in Matlab 2013a on a PC with a 2.6 GHz Intel Core CPU and 16GB RAM) and summarized in Fig. 10. The InH and EEF methods are more efficient than the RSF, WRSF and ECV methods since these two methods used edge information (see Figs. 1 and 2) obtained from the pixel inhomogeneity factor and local edge entropy, respectively. These feature information can assist to reduce unnecessary iterative evolution of contour curves in segmentation. Also, the edge entropy had better capability of handling inhomogeneity than the pixel inhomogeneity factor; hence, the proposed method was slightly better than the InH model.

4.3. Effect of local edge entropy

The developed edge entropy is an important image feature and used to construct the intensity fitting term $|L_I(x) - m_i(x)|^2$ and regularization term $\int g(x)|\nabla H(\phi(x))|dx$, respectively. This causes that the proposed method has the potential for handling intensity inhomogeneity and avoiding unnecessary contour evolution in segmentation. This can be verified by the results shown in Figs. 11 and 12, where the proposed method was tested to segment synthetic images with or without the function $g(x)$. Experiment results demonstrated that the proposed method with $g(x)$ had better segmentation accuracy and less computational cost than our method without $g(x)$ for the same images and parameters. This suggested that local edge entropy can highlight the intensity variation in an image, alleviate the problems caused by inhomogeneity, and thus assist in excluding undesirable background. With the edge entropy, the proposed method demonstrated a unique capability of handling intensity inhomogeneity.

5. Discussions

In this study, we proposed a novel active contour model to segment images and evaluated its performances based on widely used images in previous studies and a publicly available database. This model displays the capability of handling intensity inhomogeneity and achieves a relatively good segmentation accuracy and efficiency as compared to several available models, owing to the utilization of local edge entropy. There are several parameters in the proposed contour model, and some of them (e.g., σ and ε) are correlated with one another. This causes that our model has the difficulty in balancing these parameters and achieving an optimal segmentation result. For example, the parameter r is important for the local edge entropy. A small r makes edge entropy more sensitive to inhomogeneity, while a large r reduces the capability of handling inhomogeneity, and leads to the expansion of object boundaries. This can be verified by Fig. 13, where our model is capable of extracting objects of interest for the value r of 3 and 5, but fails when r is set at 7. This suggested that the developed method can achieve reasonable segmentation performances with a relatively small r value.

We are aware that there are some limitations with this method. First, although the introduction of the edge entropy makes it possible to suppress inhomogeneity in fuzzy regions and keep contour curves close to object boundaries, it may fail to highlight object boundaries and affects the segmentation accuracy of the proposed model, because pixel probabilities for the edge entropy is based on the modulus operation and its sum is generally larger than 1 in a specified region. Second, the proposed model is incompetent for certain segmentation tasks, where the desirable object depicted on an image consists of multiple components and each of them has very different intensity properties. This is caused by the fact that region based contour models are theoretically derived from the image homogeneity assumption, *i.e.*, pixel intensities should be approximately equal to one another when they present the same object in an image. This means that our model may not be suitable for segmenting natural images with large dimensions. Third, this model usually has different segmentation accuracy and robustness, depending on image resolution and contrast, and thus is inferior to certain supervised segmentation algorithms, such as convolutional neural networks (CNN) [33], which can exploit a large number of underlying texture features for precise image segmentation. To alleviate these issues of our model, we will attempt in the future to extend local edge entropy using simultaneously pixel intensities and coordinates and further improve the proposed image evaluation strategy to segment images with intensity inhomogeneity.

6. Conclusion

A region based active contour model was proposed for segmenting inhomogeneous images. Its novelty lies in the introduction of a novel feature descriptor *(i.e.,* local edge entropy), the hybrid image fitting energy functional based on pixel intensities and edge entropy, and the combination of a redefined regularization term of the level set function. Our experiments show that the developed model is capable of segmenting images with intensity inhomogeneity with a relatively high accuracy as compared to available models. This is largely attributed to the simultaneous utilization of pixel intensity and edge entropy. Also, the developed model is robust to the initial contour placement and insensitive to the presence of image noise.

Acknowledgments

This work is supported by Jiangsu Natural Science Foundation (Grant No. BK20170391), National Institutes of Health (NIH) (Grant No. R21CA197493, R01HL096613).

References

[1]. Jayadevappa D, Kumar S, Murty D, Medical image segmentation algorithms using deformable models: a review, IETE Tech. Rev 28 (3) (2011) 248–255.

[2]. Wang L, Zhu J, Sheng M, Cribb A, Zhu S, Pu J, Simultaneous segmentation and bias field estimation using local fitted images, Pattern Recognit. 74 (2018) 145–155. [PubMed: 29332955]

[3]. Mabood L, Ali H, Badshah N, Chen K, Khan G, Active contours textural and inhomogeneous object extraction, Pattern Recognit. 55 (2016) 87–99.

[4]. Le T, Savvides M, A novel shape constrained feature-based active contour model for lips/mouth segmentation in the wild, Pattern Recognit. 54 (2015) 23–33.

[5]. Caselles V, Kimmel R, Sapiro G, Geodesic active contours, Int. J. Comput. Vision 22 (1997) 61–79.

[6]. Chan T, Vese L, Active contour without edges, IEEE Trans. Image Process 10 (2) (2001) 266–277. [PubMed: 18249617]

[7]. Mylona E, Savelonas M, Maroulis D, Automated adjustment of region-based active contour parameters using local image geometry, IEEE Trans. Cybern 44 (2014) 2757–2770. [PubMed: 24771604]

[8]. Kass M, Witkin A, Terzopoulos D, Snakes: active contour models,, Int. J. Comput. Vision 1 (4) (1987) 321–331.

[9]. Xu C, Prince J, Snakes, shapes, and gradient vector flow, IEEE Trans. Image Process 7 (3) (1998) 359–369. [PubMed: 18276256]

[10]. Li C, Xu C, Gui C, Fox M, Level set evolution without reinitialization: a new variational formulation, in: IEEE Conference on Computer Vision and Pattern Recognition (CVPR), 2005, pp. 430–436.

[11]. Li C, Kao C, Gore J, Ding ZH, Implicit active contours driven by local binary fitting energy, in: IEEE Conference on Computer Vision and Pattern Recognition (CVPR), 2007, pp. 339–345.

[12]. Piovano J, Papadopoulo T, Local statistic based region segmentation with automatic scale selection, in: European Conference on Computer Vision (ECCV), 2008, pp. 486–499.

[13]. Wang L, Chang Y, Wang H, Wu Z, Pu J, Yang X, An active contour model based on local fitted images for image segmentation, Inf. Sci 418 (2017) 61–73.

[14]. Chen Y, Zhang Y, Yang J, Cao Q, Yang G, Chen J, Shu H, Luo L, Coatrieux J, Feng Q, Curve-like structure extraction using minimal path propagation with backtracking, IEEE Trans. Image Process. 25 (2) (2016) 988–1003. [PubMed: 26552086]

[15]. He C, Wang Y, Chen Q, Active contours driven by weighted region-scalable fitting energy based on local entropy, Signal Process. 92 (2012) 587–600.

[16]. Li C, Kao C, Gore J, Ding Z, Minimization of region-scalable fitting energy for image segmentation, IEEE Trans. Image Process 17 (10) (2008) 1940–1949. [PubMed: 18784040]

[17]. Dai L, Ding J, Yang J, Inhomogeneity-embedded active contour for natural image segmentation, Pattern Recognit. 48 (8) (2015) 2513–2529.

[18]. Niu S, Chen Q, Sisternes L, Ji Z, Zhou Z, Rubin D, Robust noise region-based active contour model via local similarity factor for image segmentation, Pattern Recognit. 61 (2017) 104–119.

[19]. Mumford D, Shah J, Optimal approximations by piecewise smooth functions and associated variational problems, Commun. Pure Appl. Math 42 (5) (1989) 577–685.

[20]. Shiozaki A, Edge extraction using entropy operator, Comput. Vision Graphics Image Process 36 (1) (1986) 1–9.

[21]. Wang L, Zhang H, He K, Chang Y, Yang X, Active contours driven by multi-feature Gaussian distribution fitting energy with application to vessel segmentation, PLoS ONE (2015) 16.

[22]. Zheng Q, Dong E, Cao Z, Sun W, Li Z, Active contour model driven by linear speed function for local segmentation with robust initialization and applications in MR brain images, Signal Process. 97 (2014) 117–133.

[23]. Zhang K, Zhang L, Song H, Zhou W, Active contours with selective local or global segmentation: A new formulation and level set method, Image Vision Comput. 28 (2010) 668–676.

[24]. Badshah N, Chen K, Ali H, Murtaza G, Coefficient of variation based image selective segmentation model using active contours, East Asian J. Appl. Math 2 (2) (2012) 150–169.

[25]. Zhang K, Liu Q, Song H, Li X, A variational approach to simultaneous image segmentation and bias correction, IEEE Trans. Cybern 45 (8) (2015) 1426–1437. [PubMed: 25347891]

[26]. Wang L, He L, Mishra A, Li C, Active contours driven by local Gaussian distribution fitting energy, Signal Process. 89 (2009) 2435–2447.

[27]. Li C, Xu C, Gui C, Fox M, Distance regularized level set evolution and its application to image segmentation, IEEE Trans. Image Process 19 (12) (2010).

[28]. Ji Z, Xia Y, Sun Q, Cao G, Chen Q, Active contours driven by local likelihood image fitting energy for image segmentation, Inf. Sci 301 (2015) 285–304.

[29]. Wang L, Li C, Sun Q, Xia D, Kao C, Active contours driven by local and global intensity fitting energy with application to brain MR image segmentation, Comput. Med. Imaging Graphics 33 (2009) 520–531.

[30]. Zhang K, Zhang L, Lam K, Zhang D, A level set approach to image segmentation with intensity inhomogeneity, IEEE Trans. Cybern 46 (2) (2016) 546–557. [PubMed: 25781973]

[31]. Zhang K, Song H, Zhang L, Active contours driven by local image fitting energy, Pattern Recognit. 43 (4) (2010) 1199–1206.

[32]. Chen Y, Zhang Y, Shu H, Luo L, Coatrieux J, Feng Q, Structure-adaptive fuzzy estimation for random-valued impulse noise suppression, IEEE Trans. Circuits Syst. Video Technol (99) (2016).

[33]. Litjens G, Kooi T, Bejnordi B, Setio A, Ciompi F, Ghafoorian M, Laak B J Ginneken, C. Sanchez, A survey on deep learning in medical image analysis, Med. Image Anal 42 (2017) 60–88. [PubMed: 28778026]

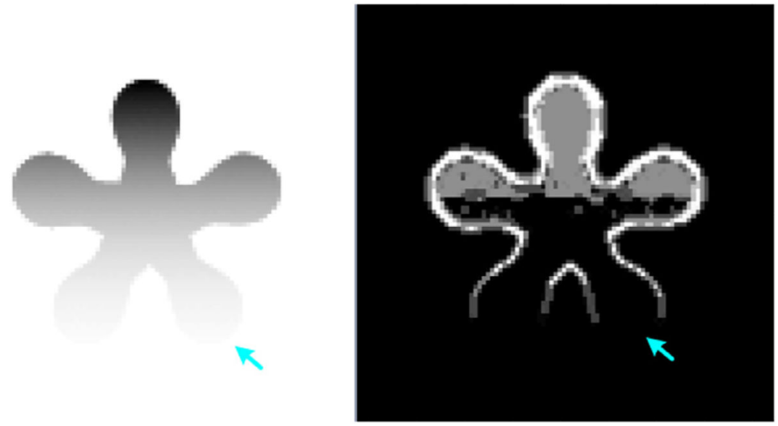

Fig. 1.

The right is the feature map of a given image in the left, which is obtained by pixel inhomogeneity factor based on a circle window with a diameter of 5 (pixels). The feature failed to identify target objects in the region as indicated by the arrow.

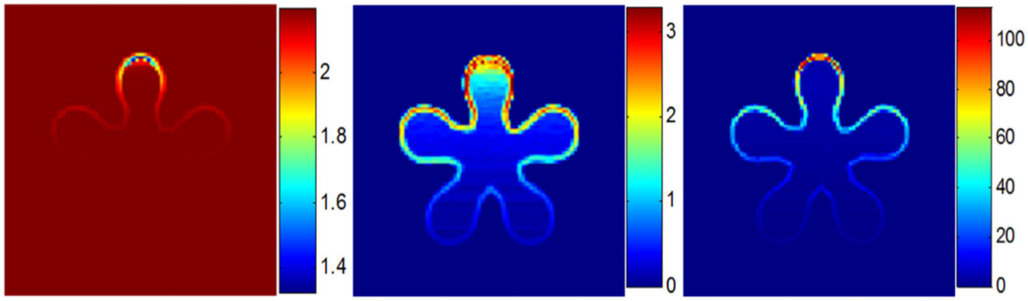

Fig. 2.

Feature maps obtained using Shiozaki's entropy (left) and the proposed entropy (center) based on a circle window with a diameter of 3 (pixels) for the image shown in Fig. 1. The image gradients are shown in the right.

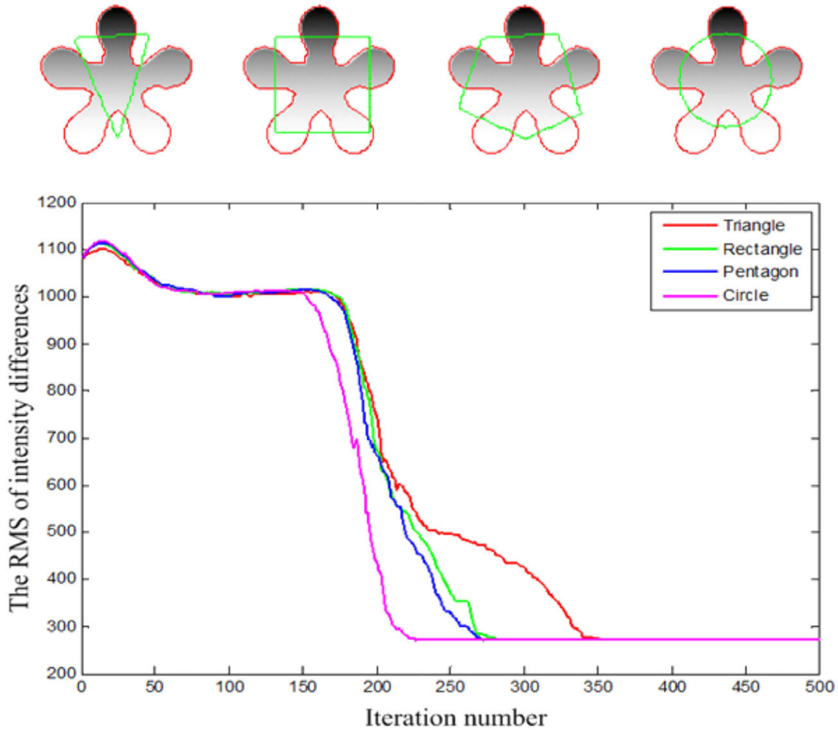

Fig. 3.

Segmentation results of an inhomogeneous image by the proposed method for different initial contours. The top row is the initial contours (in green) and their final results (in red), the bottom row shows the RMS of intensity differences between the original image and its local fitted image [31] with respect to iteration numbers. (For interpretation of the references to colour in this figure legend, the reader is referred to the web version of this article.)

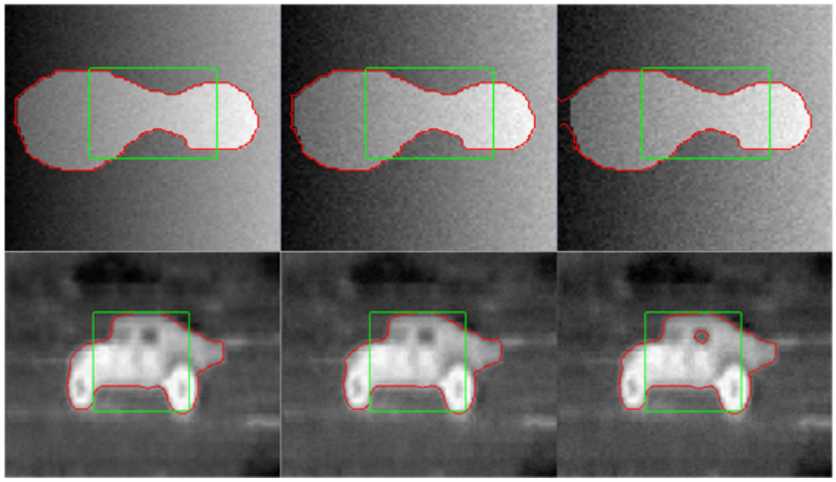

Fig. 4.

Segmentation results of the developed method for two images corrupted by different Gaussian noise [32]. From left column to right one are images with different levels of noise (standard deviations: 5, 10, and 15, respectively).

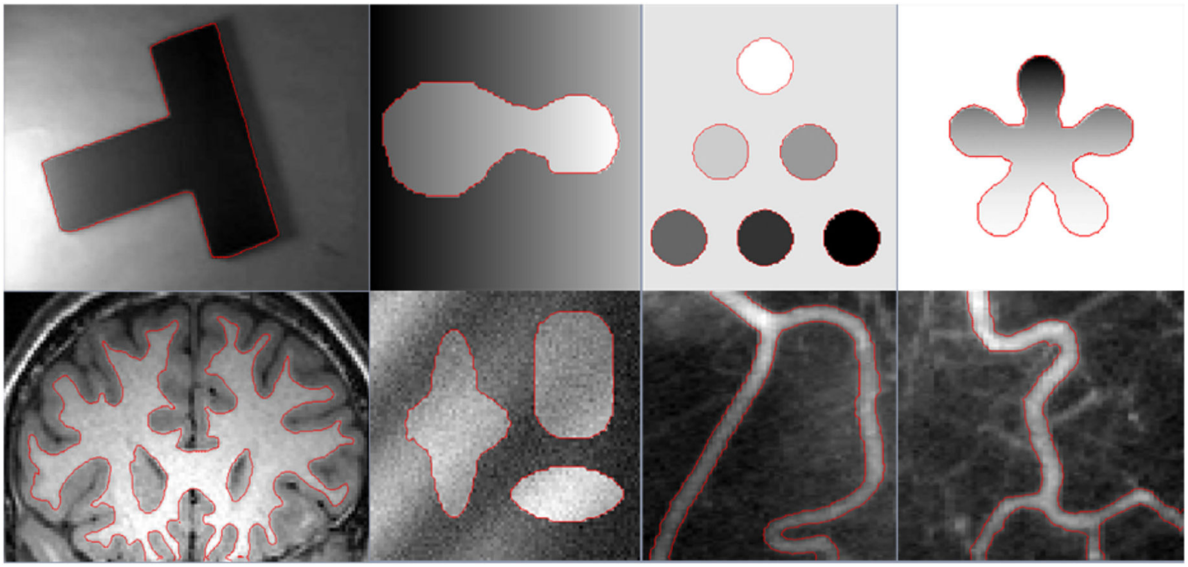

Fig. 5.

The segmentation results of the proposed method for eight test images with different noise and inhomogeneity.

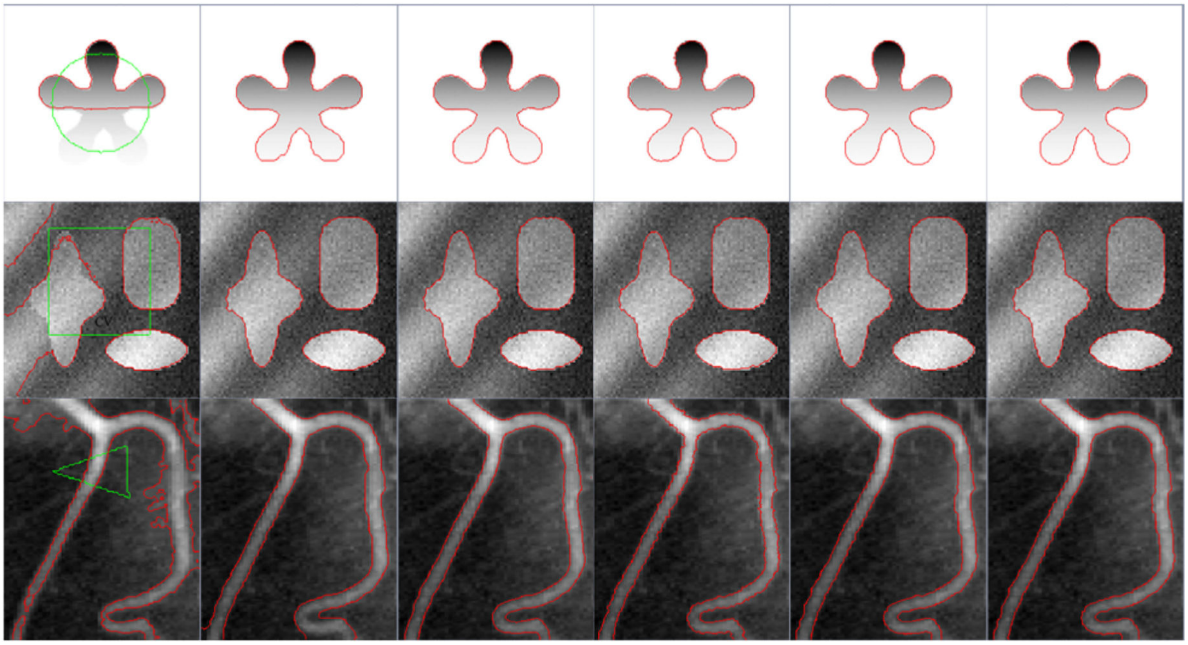

Fig. 6.

Segmentation results of three inhomogeneous images obtained separately by the CV, RSF, WRSF, InH, ECV and EEF methods in different columns.

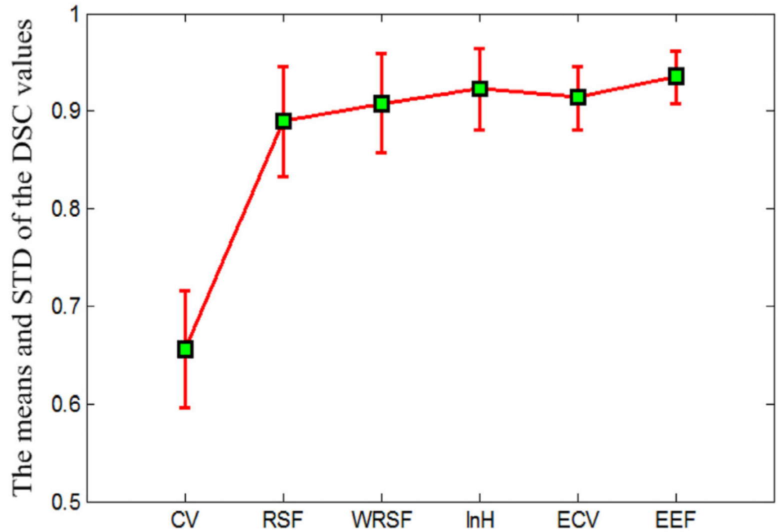

Fig. 7.
The means and standard deviations of the DSC values for six different methods based on images shown in Fig. 5.

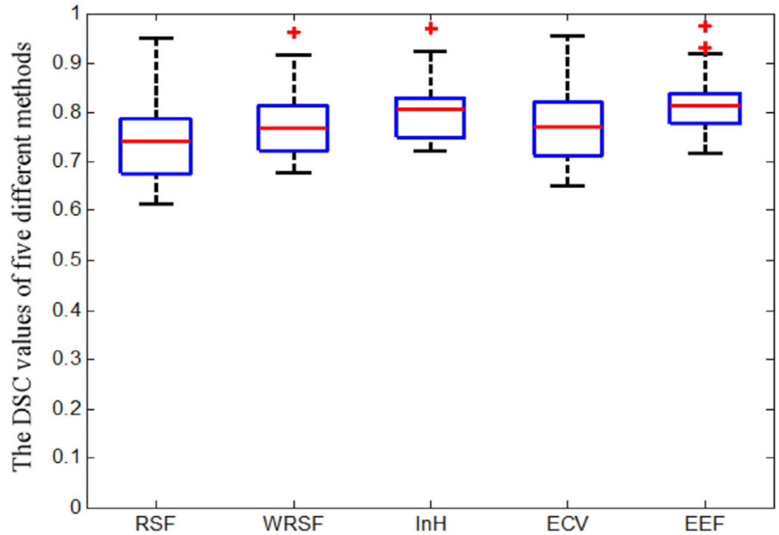

Fig. 8.

The DSC values of the RSF, WRSF, InH, ECV and our methods based on 35 randomly chosen natural images from BSD500 dataset.

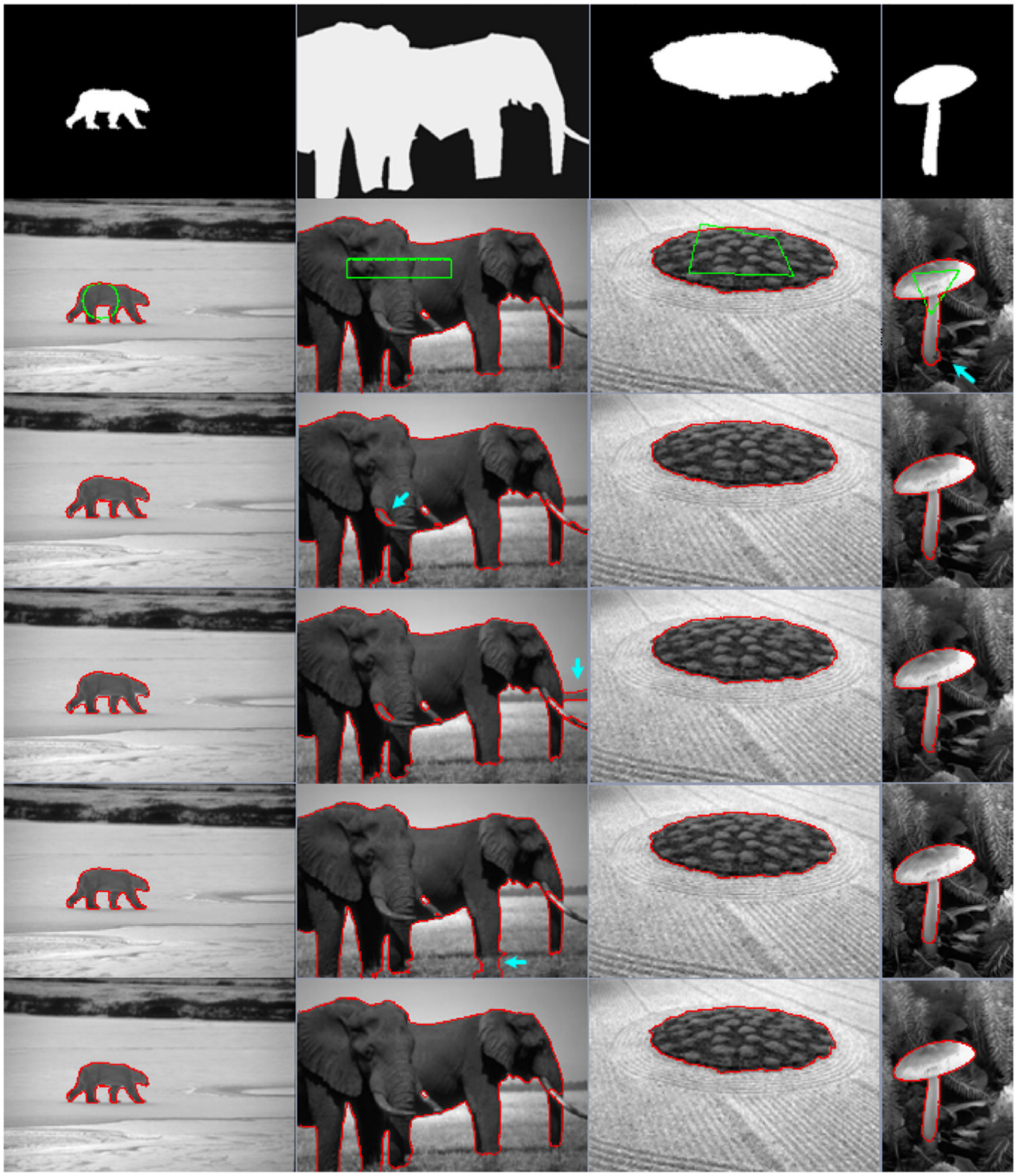

Fig. 9.

Comparisons of segmentation results obtained by the RSF, WRSF, InH, ECV, and our methods for different initial contours (in green). From top row to bottom one corresponds to the manual annotations and the results of the RSF, WRSF, InH, ECV and our methods, respectively. (For interpretation of the references to colour in this figure legend, the reader is referred to the web version of this article.)

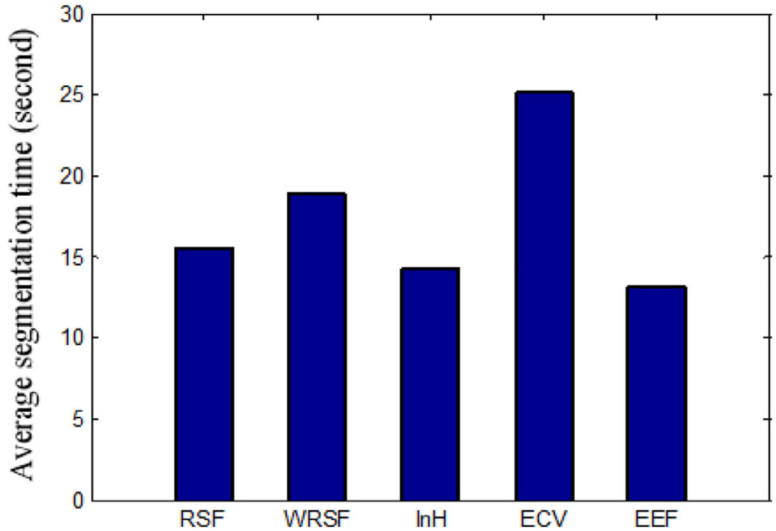

Fig. 10.
The average computational cost of the RSF, WRSF, InH, ECV and EEF models based on all of test images.

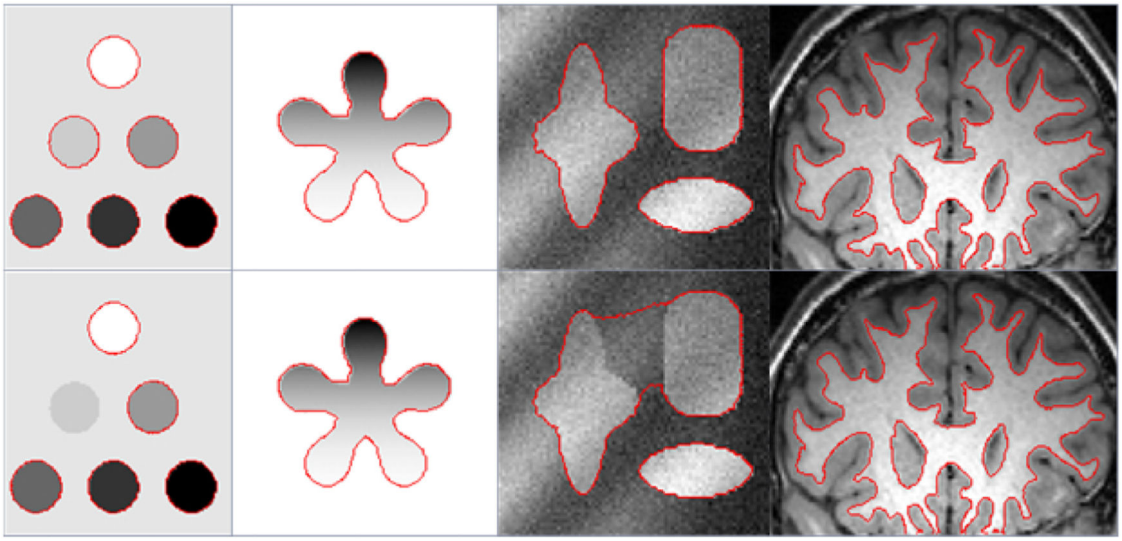

Fig. 11.

Segmentation results of the developed model with (1st row) and without (2nd row) the function $g(x)$ for images shown in Fig. 5.

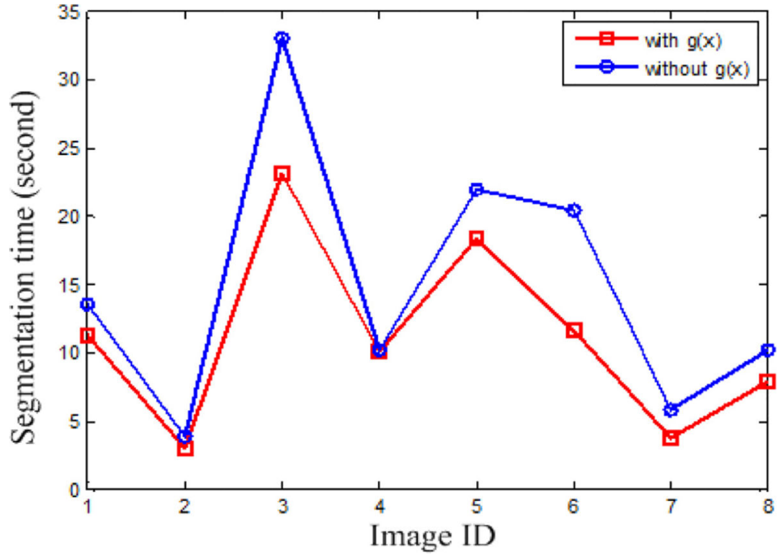

Fig. 12.

The computational cost of the proposed method with or without $g(x)$ for eight images shown in Fig. 5, where images in the first and second rows were numbered from 1 to 4, and 5 to 8, respectively.

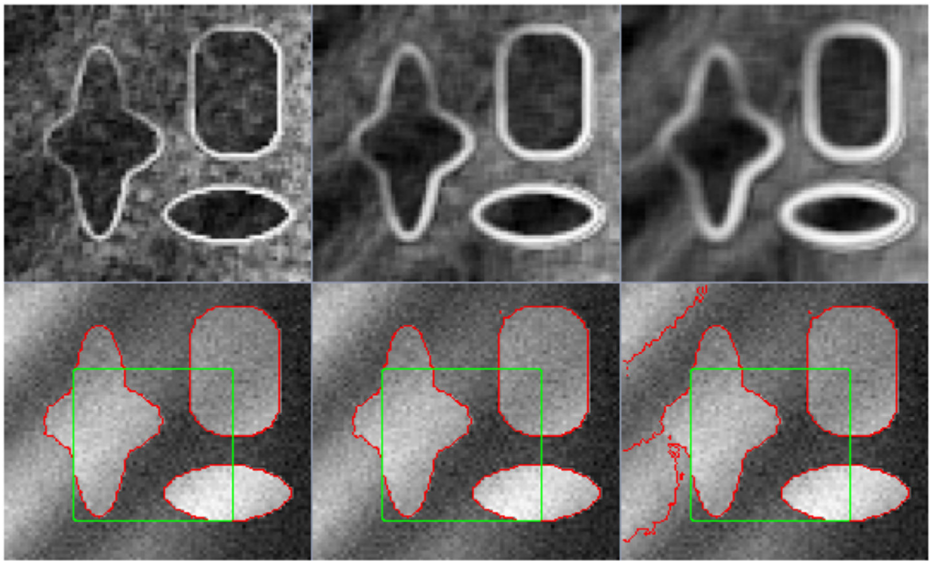

Fig. 13.

Segmentation results of the proposed method for different edge entropies. The top row displays the edge entropy with the value r of 3, 5, and 7, respectively, the bottom row is the initial (in green) and final (in red) contours. (For interpretation of the references to colour in this figure legend, the reader is referred to the web version of this article.)